



Research Article

Hall current's effect on MHD boundary layer compressible flow of fluid past a stretching sheet with viscous dissipation

Bandita DAS¹, Sunmoni MUDOI^{2,*}, Dipak SARMA²

¹Department of Mathematics, Guwahati College, Guwahati, 781021, India

²Department of Mathematics, Cotton University, Guwahati, 781001, India

ARTICLE INFO

Article history

Received: 21 July 2024

Revised: 18 September 2024

Accepted: 28 November 2024

Keywords:

bvp4c; Hall Current; Heat Transfer; MHD; Viscous – Dissipation

ABSTRACT

This work investigates the consequence of hall current on the boundary layer along a stretching sheet in the occurrence of magnetohydrodynamics, heat transfer and viscous dissipation. In the direction of the flow, a uniform transverse magnetic field is applied. Here, the controlling equations are modified into nonlinear ordinary expressions, implementing the similarity transformation. Validation is accomplished by applying the MATLAB bvp4c skill. We then visually display the impact of varied parameters by introducing temperature and non-dimensional velocity into the problem. Moreover, it is found that the relevant parameters significantly affect the flow patterns and other important physical quantities by organizing and categorizing their effects on the coefficients of skin-friction and heat transfer rate using the Nusselt number, which are of concrete relevance. Our study shows that increasing the Hall current parameter results in an enhanced primary velocity flow pattern, accompanied by a reduction in secondary velocity and temperature flow patterns.

Cite this article as: Das B, Mudoi S, Sarma D. Hall current's effect on MHD boundary layer compressible flow of fluid past a stretching sheet with viscous dissipation. Sigma J Eng Nat Sci 2026;44(1):318–328.

INTRODUCTION

A basic idea in fluid dynamics, laminar boundary layer flow specifies how a fluid behaves when it passes over a solid surface with layers that are smooth and organized. Every layer of the fluid slides easily over the layer below it in this kind of flow, which is composed of parallel layers. Laminar boundary layer flow is very important to engineers working on heat transfer surfaces, pipes, and air-plane wings and laminar boundary layer flows have been

comprehensively reviewed by various researchers, offering a deep understanding of a key aspect of fluid mechanics to the research community [1–4]. Boundary layer flows over a continuous surface of a solid body have been comprehensively reviewed by a variety of researchers, each contributing to our knowledge base in different aspects, including fundamental theories, mechanisms and theories of stability and transition, control techniques, effects of surface conditions, numerical analysis, experimental techniques, and inter/multidisciplinary studies, among others, of boundary

*Corresponding author.

*E-mail address: sunmoni77.mudoi@gmail.com

This paper was recommended for publication in revised form by Editor-in-Chief Ahmet Selim Dalkilic



layer flows associated with or involving boundary layer flows on continuous surfaces of solid bodies, like the body of an airplane, the fuselage of an airplane, or airplane wings, among other aerospace surface structures and other bodies like tanks and buses, among other applications [5,6]. The effects of heat radiation on gray fluids that absorb and emit near a black vertical plate were studied by Cess [7].

Unsteady free convective transport accompanied by MHD mass transfer along a vertical porous plate is an interesting phenomenon to explore and has numerous applications in environmental sciences, engineering, and physics. To understand phenomena of plasmas, core dynamics of the Earth, and metal liquids in industries, it is necessary to understand the nature of the magnetohydrodynamic fluids or MHD. It leads to more complex fluid dynamics and is used in heat transfer systems and cooling systems accompanied by free convection currents and is induced by density differences caused by fluid temperatures. Taking into account the diffusion of chemicals within the fluid leads to more complex dynamics because of the inclusion of mass transfer. It is necessary to understand the dynamics of mass transfer because of its applications in environmental pollution and other different applications in the field of chemical engineering. In general, exploring magnetohydrodynamic unsteady free convection transport together along with a vertical porous plate increases our understanding of fluid dynamics and is used in different applications in the field of technology. Numerous researchers [8–11] have investigated the dynamics of forced and natural convection present in magnetohydrodynamic transport. Similarity analysis on the boundary layer forced and natural convection of incompressible fluid was first proposed by Ferdows [12]. The study focused on the flow process in a non-conducting porous plate.

Stretching sheets are prepared by elongating a film of a polymeric material. This is a widely relevant topic in a polymeric industrial setup. Some of the applications of this technology involve preparation of films, packing, or even textiles. This operation of sheet stretching is a widely important aspect of tailoring materials for a specific application, and it helps a great deal in altering the properties of a particular material considerably. Stretching sheets are used within the polymeric industry for making a number of products such as shrink wraps, tapes, food packing plastic films, or synthetic fibers for textiles [13–16].

Quality of product can be largely affected if there is variation in the rate of cooling. Moreover, through the application of electrically conductive fluids within a magnetic field, control over the rate of cooling can be easily exercised. This will make it relatively simpler to provide the desired properties to the product. In order to study and ensure the desired product quality, one requires complete knowledge about heat transfer. In case of radiative heat transfer of a complex nature inside a medium located around specular reflectors, the medium interacts with the radiation in different manners such as scattering, emission, and absorption.

The heat transfer rate can be enhanced through the confinement of radiation within the medium using spherical reflectors. In order to provide better thermal performance for an efficient rate of heat transfer as observed in practical applications such as solar energy collection systems as well as thermal insulation systems, it is essential to make proper modifications in the design of specular reflectors and control the properties of the medium involved [17–21].

Hall currents affect fluid flow immensely in various applications, but their importance is most prominent in magnetohydrodynamics (MHD) applications, where magnetic fields are applied to electrically conductive fluids. There will be additional forces acting on the fluids when the Hall current is also taken into consideration, as it depends upon the combined effects of the electric current and the magnetic field applied. Various applications of engineering, such as the production of power using MHD, semiconductor devices, plasma research, and microfluidics, all involve knowing the effects of Hall currents on the flow of fluids. The effect of the Hall current on an unsteady natural convection flow is explained by Sattar and Hossain [22]. They took into account the concentration and plate temperature as time-dependent variables. The properties of mass transfer and stable double-diffusive free convective heat in a chemically-reacting micropolar fluid were investigated by Beg [23].

A stretching sheet is a flat surface that expands or stretches in a single direction at a speed proportional to its distance from the origin. If a fluid flows through a stretched sheet in a continuous two-dimensional hydromagnetic flow, things like the effect of magnetic fields, fluid dynamics, and behavior of boundary layer become very important to the study. Recent research has investigated the constant two-dimensional hydromagnetic flow of a fluid past a stretching sheet. The effects of viscous and Joule dissipations on the flow characteristics were the focus of the enquiry [24]. The work introduced the aspects of Brownian motion in the transport equations. The repercussions of diffusion-thermo and thermal-diffusion on the axisymmetric magnetohydrodynamic flow were studied by Hayat and Hendi [25]. They used the HAM method to inspect the implications of viscous dissipation, Joule heating, Hall and ion-slip currents, and a first order chemical process. The problem was scrutinized by running the Chebyshev collocation method jointly with the successive linearization method (SLM) considering variable thermal diffusivity, Hall and ion-slip currents, and chemical reaction. Marin [26–28] has reviewed a great deal on materials' thermoelectricity and micropolar bodies. Ferdows et al. [29] have investigated the impact of Hall current and viscous dissipation on boundary layer flow.

This study investigates the effect of various parameters in natural convection in the presence of a strongly magnetic field on a stretching sheet. It focuses on the aspects of heat transfer and boundary layer flow. This study aims to integrate the dynamic effect of hall currents and viscous

dissipation. The equations, numerical method, and mathematical modeling required for simulation are described later on.

MATHEMATICAL DESCRIPTION

We study the behavior of an electrically conducting, incompressible, viscous, and stable fluid moving in the x-direction down a vertical surface while taking heat transfer into account. As illustrated in Figure 1, the flow is further influenced by a strong magnetic field B_0 of constant intensity oriented along the y-axis. As a stretching sheet gets farther from the leading edge, its velocity component \bar{u} , changes proportionally. Here, the velocity components in the x, y and z direction are, respectively, \bar{u} , \bar{v} , and \bar{w} .

An electrically conducting fluid is typically affected by Hall current when a magnetic field is present. Because of the Hall current effect, there is a force in the z-direction, which causes a cross-flow and makes the flow three-dimensional. $J_y = \text{constant}$ is the result of the conservation of charge equation $\nabla \cdot \vec{J} = 0$, where the current density is $\vec{J} = (J_x, J_y, J_z)$. $J_y = 0$ at the plate and hence everywhere since this constant is zero because the plate is non-conducting.

To simplify the problem, we assume that the amounts of heat transfer and flow in the z-direction are constant. By using the standard boundary layer theory, Boussinesq approximations and the previously indicated assumptions, the governing boundary layer equations can be formulated as follows:

$$\bar{u}_x + \bar{v}_x = 0 \tag{1}$$

$$\bar{u}\bar{u}_x + \bar{v}\bar{u}_y = \nu\bar{u}_{yy} + \bar{u}\bar{e}\bar{u}_{e_x} + g^*\beta^*(\bar{T} - \bar{T}_\infty) - \frac{\bar{B}_0}{\rho}J_z \tag{2}$$

$$\bar{u}\bar{w}_x + \bar{v}\bar{w}_y = \nu\bar{w}_{yy} + \frac{\bar{B}_0}{\rho}J_x \tag{3}$$

$$\begin{aligned} \bar{u}\bar{T}_x + \bar{v}\bar{T}_y &= \frac{k}{\rho c_p}\bar{T}_{yy} + \frac{\nu}{c_p}((\bar{u}_y)^2 + (\bar{w}_y)^2) \\ &+ \frac{\sigma\mu_e\bar{B}_0^2\lambda}{\rho c_p(1+m^2\lambda^2)}(u^2 + w^2) \end{aligned} \tag{4}$$

Physical Boundary Conditions

$$\text{At } y=0, \bar{u} = u_0 = Bx, \bar{v} = 0, \bar{w} = 0, \bar{T} = \bar{T}_w = \bar{T}_\infty + A\left(\frac{x}{l}\right)$$

$$\text{As } y \rightarrow \infty, \bar{u} = \bar{u}e(x) = Cx, w \rightarrow 0, \bar{T} \rightarrow \bar{T}_\infty \tag{5}$$

Similarity Analysis

$$\begin{aligned} \eta &= y\left(\frac{B}{\nu}\right)^{\frac{1}{2}}, \bar{u} = Bxf'(\eta), \bar{v} = -(B\nu)^{\frac{1}{2}}f(\eta), \\ \bar{w} &= Bxg(\eta) \text{ and } \theta(\eta) = \frac{\bar{T} - \bar{T}_\infty}{\bar{T}_w - \bar{T}_\infty} \end{aligned} \tag{6}$$

Transformed equations

$$f''' + ff'' - f'^2 + \delta^2 + Gr^*\theta - \frac{M\lambda}{m^2\lambda^2 + 1}(f' + mg\lambda) = 0 \tag{7}$$

$$g'' + g'f + gf' + \frac{M\lambda}{m^2\lambda^2 + 1}(mf'\lambda - g) = 0 \tag{8}$$

$$\theta'' + \theta'fPr - \theta f'Pr + \frac{M\lambda}{m^2\lambda^2 + 1}Ec.Pr(g^2 + f'^2) = 0 \tag{9}$$

The modified boundary conditions are as follows:

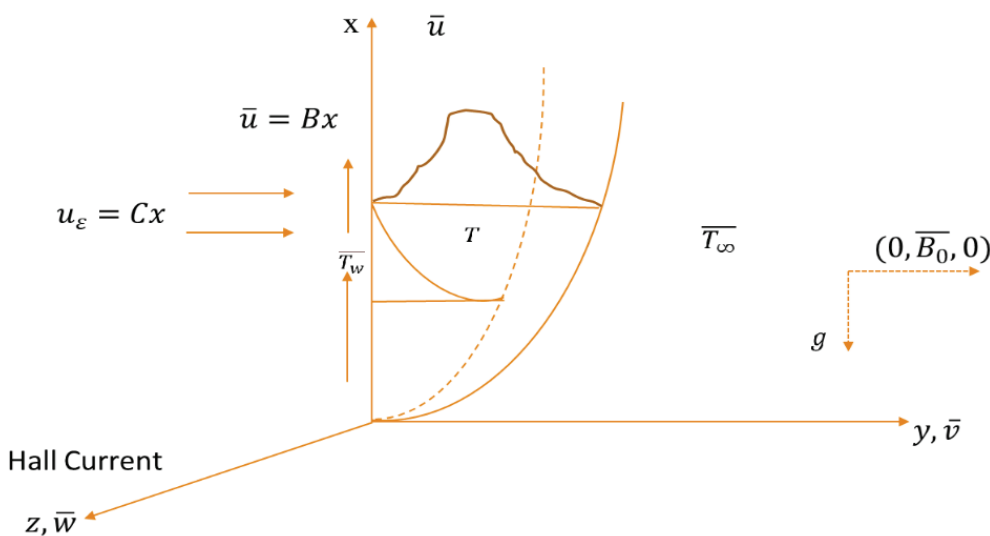


Figure 1. Geometrical model.

$$f(0) = 0, f'(0) = 1, g(0) = 0, \text{ and } \theta(0) = 1$$

$$f' \rightarrow \delta, g \rightarrow 0, \theta \rightarrow 0 \quad \text{as } \eta \rightarrow \infty \quad (10)$$

MATERIALS AND METHODS

To solve equations (7), (8), and (9) while adhering to the restriction outlined in condition (10), we will now utilise the bvp4c approach. It is a mathematical method that MATLAB has built-in. For the various parameters, the temperature coefficient and velocity graph findings are explained in detail.

To apply finite difference-based solver bvp4c the dimensionless equations (7)- (9) respectively transformed as:

$$\begin{aligned}
 f &= y1; f' = y1' = y2; f'' = y2' = y3 \\
 g &= y4; g' = y4' = y5; \theta = y6, \quad \theta' = y6' = y7 \\
 y3' &= -y1 * y3 + 2 * y2^2 - \delta^2 - Gr * y6 + \left(\frac{m\lambda}{m^2 * \lambda^2 + 1}\right) * (y2 + m * y4 * \lambda) \\
 y5' &= -y5 * y1 - y4 * y2 - \left(\frac{m\lambda}{m^2 * \lambda^2 + 1}\right) * (m * y2 * \lambda - y4) \\
 y7' &= -Pr * \left(y1 * y7 - y6 * y2 + \left(\frac{m\lambda}{m^2 * \lambda^2 + 1}\right) * Ec * (y4^2 + y2^2)\right)
 \end{aligned}$$

Also, initial and boundary conditions (10) are transformed:

$$\begin{aligned}
 y1(0) &= 0; y2(0) = 1; y4(0) = 0; y6(0) = 1 \\
 y2(\infty) &= \delta; y4(\infty) = 0; y6(\infty) = 0
 \end{aligned}$$

These transformed results are used in MATLAB to perform the numerical computation of the solution.

RESULTS AND DISCUSSION

We explore the physical consequence of several critical parameters on the temperature distribution, secondary flow distribution, and primary flow distribution in this section. Magnetic parameter (*M*), Grashof number (*Gr*), Hall current (*m*), Prandtl number (*Pr*) are the parameters of interest. Figures 2-16 shows the graphical depictions of these impacts.

Effects of Prandtl Number

The temperature and momentum boundary layers proportional thickness are described by a dimensionless number called the Prandtl number. The ratio of momentum diffusivity to heat diffusivity can be used to express it.

Comparing thermal diffusivity with momentum diffusivity, the former is smaller for high values of *Pr*. Consequently, there is a higher momentum boundary layer compared to a lower temperature boundary layer. Lower

primary flow velocity ensues from the fluid experiencing higher resistance to motion. The motion of fluid is slower nearer the boundary; this is evidenced by a steeper velocity gradient which approaches the wall. On the contrary, when *Pr* is smaller, thermal diffusivity is higher than the momentum diffusivity. In this case, the fluid can move more freely because the momentum boundary layer is thinner than the temperature boundary layer. This leads to a less steep velocity gradient near the wall and thus a higher primary flow velocity. Globally, the secondary flow is less influenced by *Pr* than the primary flow is influenced by it. However, there may still be an effect from the differences in Prandtl number on the global stability and structure of flow. Due to higher viscosities, a large *Pr* number could dampen secondary flow or a small *Pr* number could enhance secondary flow through reduced viscous resistance. Higher *Pr* number: Sharp velocity gradient near the wall, small momentum boundary layer, and localized fluid flow. Smaller *Pr*, faster fluid flow, a large momentum boundary layer, and a gradual velocity gradient region close to the wall. More severe temperature gradient close to the wall, small thermal boundary layer, smaller temperature gradient for higher *Pr*, and localized conduction. Less severe temperature gradient close to the wall, large thermal boundary layer, and diffused conduction. Figures 2-4 describe Prandtl number effects on primary, secondary, and temperature profiles.

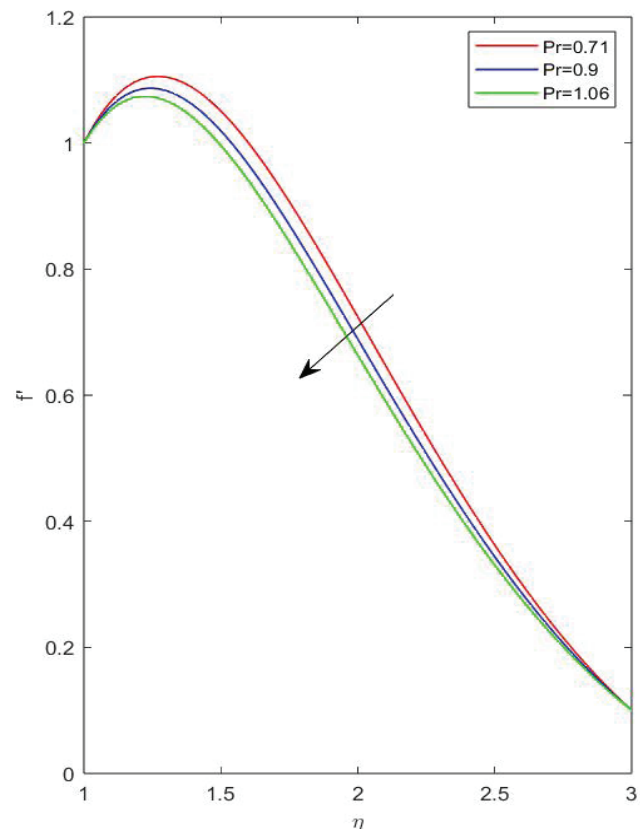


Figure 2. Primary velocity flow patterns for *Pr*.

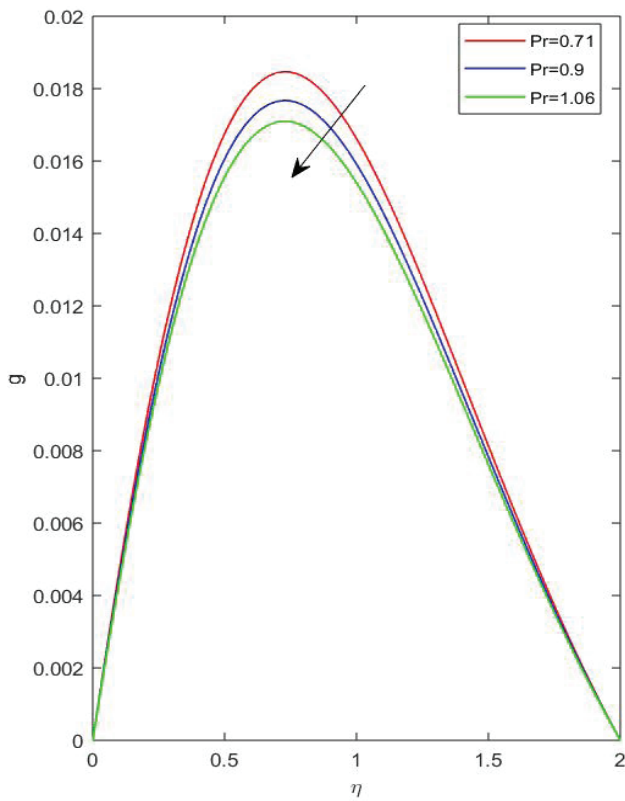


Figure 3. Secondary velocity flow patterns for Pr.

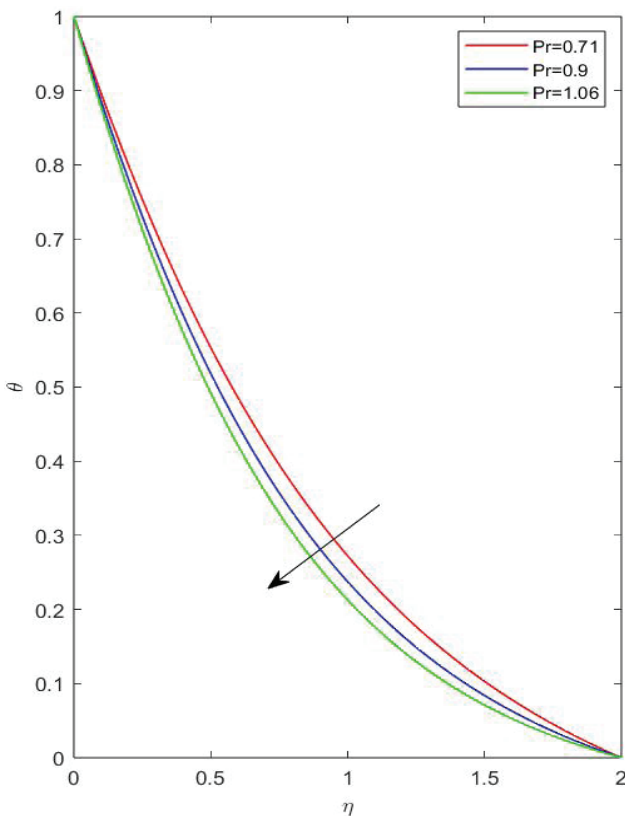


Figure 4. Temperature variations for Pr.

Effect of Magnetic Parameter

One of the significant aspects of fluid dynamics, especially in the context of magnetohydrodynamics, is the effect of the magnetic parameter on the velocity profile.

The main velocity in MHD fluids is considerably affected by the presence of the magnetic parameter, which is named the Hartmann number. The increase in the magnetic damping corresponding to a larger value of the parameter M , results in a homogeneous velocity profile and a reduced boundary layer. This similarity in the velocity profile, from a parabolic to a flat profile, highlights the significance of the magnetic field in the control of fluid velocity in MHD processes. The velocity perpendicular to the principal direction of the principal velocity, normally because of the emergence of the magnetic field, is named the velocity profile of the second kind in MHD. For the use of MHD pumps, generators, and the control of the fluid process in various engineering systems, it is necessary to understand the penetration of the magnetic parameter in the second velocity profile of the MHD process. The second velocity profile of the MHD process is immensely influenced by the magnetic parameter. A flat velocity profile occurs in the middle region of the process, and a high velocity gradient occurs in the boundary layer as the magnetic parameter, m ,

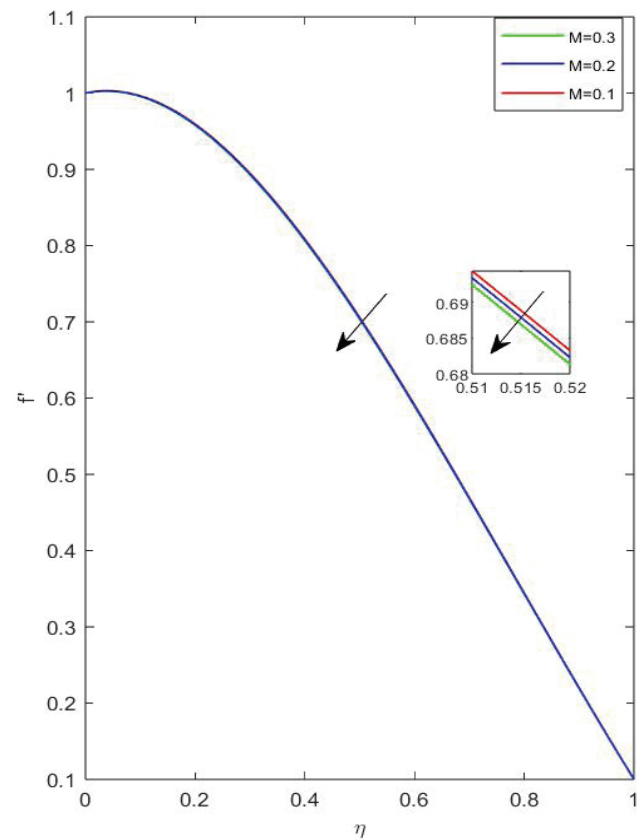


Figure 5. Primary velocity flow patterns for Magnetic parameter (M).

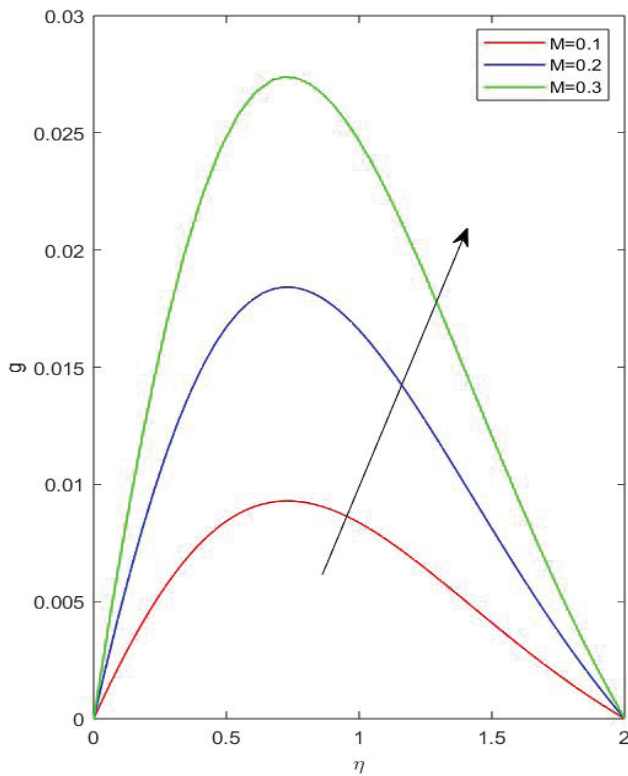


Figure 6. Secondary velocity flow patterns for magnetic parameter.

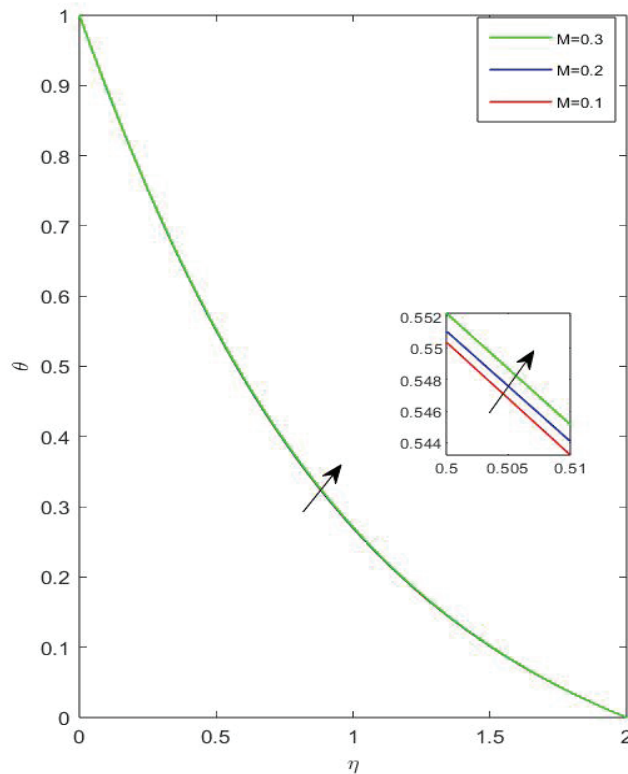


Figure 7. Temperature variations for magnetic parameter.

increments due to intensified magnetic damping, accompanied by a decrement in the second velocity.

In many technical and commercial applications, the impact of the magnetic parameter on the temperature flow patterns in MHD flows is crucial to take into account. Due to variations in flow dynamics and heat transfer properties, the existence of a magnetic field affects both the velocity and the temperature flow patterns.

The effects of the magnetic parameter on the primary velocity flow patterns, secondary velocity flow patterns, and temperature distribution are shown, respectively, in Figures 5-7.

Effects of Hall Current

The behavior of the primary, secondary, and temperature distribution in MHD is further complicated by the Hall effect, which arises when a magnetic field is applied at right angled to the flow of an electrically conducting fluid. Because of the way the magnetic field and fluid motion interact, the Hall current can drastically change these characteristics.

In Magnetohydrodynamic flows, the main velocity, secondary velocity, and temperatures are strongly affected by the Hall current given by the following equations:

The main velocity is impacted by the inclusion of potential asymmetries and the change of the Lorentz force because of the Hall current. Because of the induced currents that are opposite to the magnetic field and the main flow, the secondary velocity is amplified and could possibly have more complexity. Because of the induced currents that are opposite to the magnetic field and the main flow, the secondary velocity is amplified and could possibly have more complexity. There could be effects of raised local temperatures and differences in the thermal boundary layers because of changes in the temperature profile owing to differences in the convective heat transfer and Joule heating.

The effects of the Hall parameter on the primary velocity flow patterns, secondary velocity flow patterns, and temperature distribution are shown, respectively, in Figures 8-10.

Effect of Grashof Number

A dimensionless integer called Grashof number, Gr, denotes the relative significance of buoyancy force to viscous force in fluid mechanics and conduction of heat. The following description illustrates the significance of the Grashof number in different ways, concerning the phenomenon of natural convection, a type of fluid motion driven by buoyancy force:

Main Velocity Profile: The main velocity profile would show the fluid moving upwards in the vicinity of the heated surface and subsequently moving downwards in the opposite direction. The Grashof number depends on this. The buoyant force will be large when there is a higher velocity, which is expressed through the Grashof number.

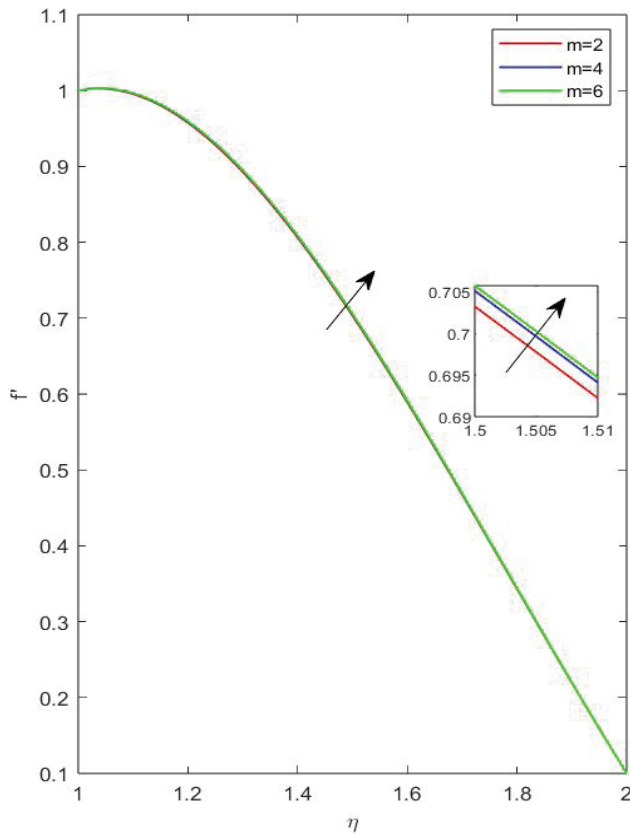


Figure 8. Primary velocity flow patterns for hall current (m).

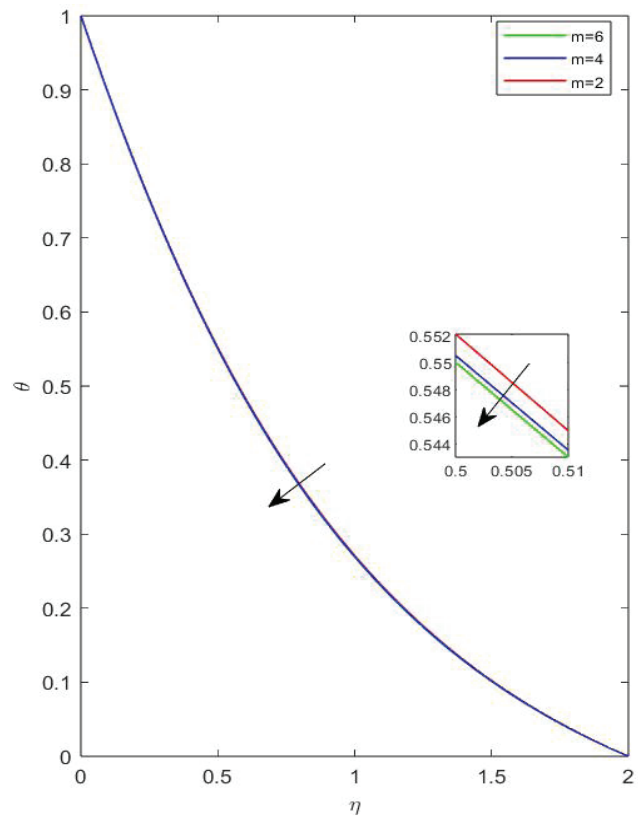


Figure 10. Temperature variations for hall current (m).

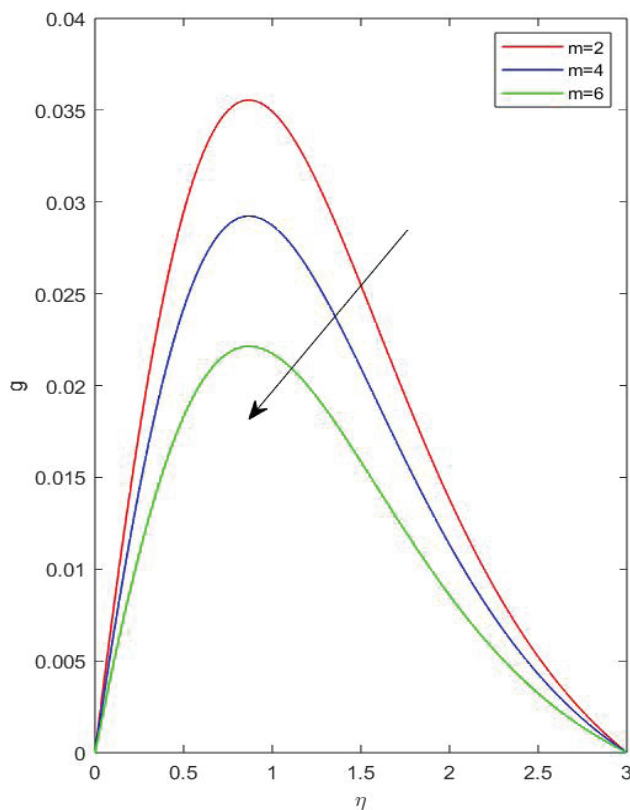


Figure 9. Secondary velocity flow patterns for hall current (m).

Secondary Velocity Profile: The presence of any obstruction to the flow direction, such as walls or other obstructions, may produce a couple with the principal buoyancy-driven flow, giving rise to secondary flows, swirls, and vortices. The intensity and nature of the secondary flows are functions of the Grashof number.

Temperature Profile: The Gr, or Grashof number, too has its say in the temperature profile for free convection. Since more fluid is moved due to buoyancy forces, a higher Grashof number leads to a more apparent temperature gradient and results in a higher heat transfer rate. Therefore, the temperature of the fluid will distribute more uniformly far away from the heated surface and steeper near it.

As one can conclude, the Grashof number affects both the temperature profile and the primary and secondary velocity flow patterns in fluid movement due to natural convection. Larger buoyancy effects would lead to more energetic fluid motion and, therefore, enhanced heat transmission, which can be demonstrated by higher Grashof values. Figures 1-13 present both the primary and secondary velocity profiles and the temperature distribution for different Gr values.

Table 1 demonstrates the validity of our work in comparison to some previously published research. Here, we compare the heat transfer rate values for various parameters with those from published papers. We see that our work is valid with some previously published

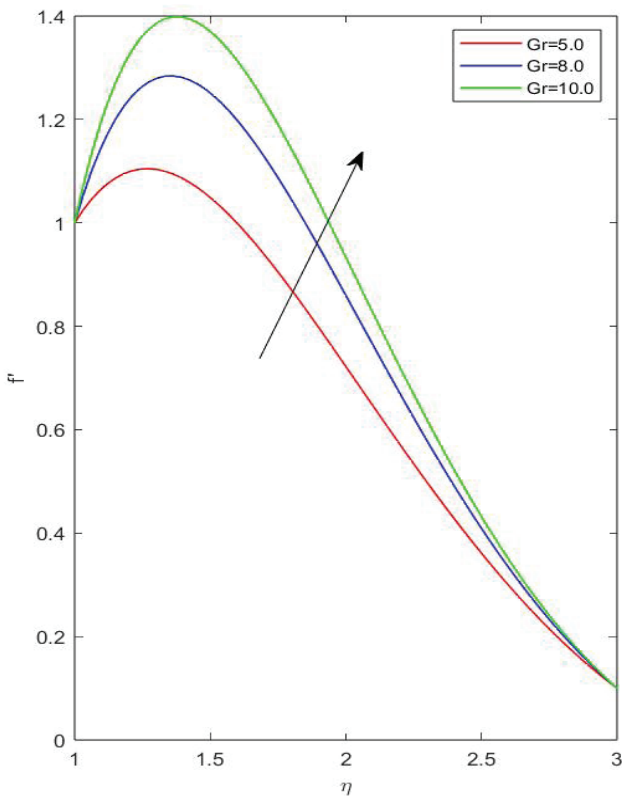


Figure 11. Primary velocity flow patterns for grashof number.

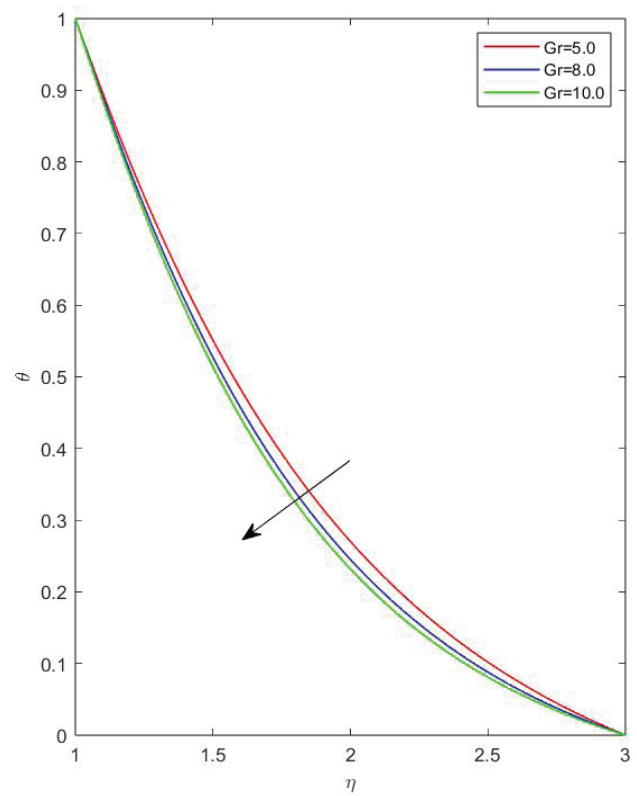


Figure 13. Temperature variation for grashof number.

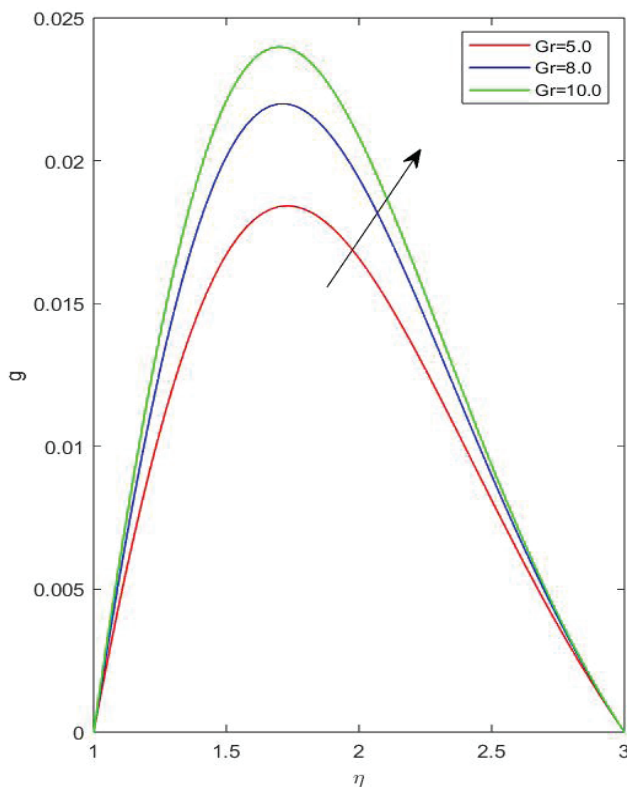


Figure 12. Secondary velocity flow patterns for grashof number.

papers. Lastly, Table 2. shows the consequences of several scientific parameters that arose at the plate surface in the problem, including skin frictions caused by primary and secondary velocity ($C_{fx} \propto f''(0)$ and $C_{fz} \propto g'(0)$) and the Nusselt number ($Nu_x \propto -\theta'(0)$). Skin friction is increased with increasing m , Ec , Gr , and δ and decreased with increasing M and Pr . Raising the skin friction coefficient causes the surface to experience more shear stress, higher drag force, and improved fluid-surface momentum transfer. It causes a greater pressure drop, a lower flow rate, more drag, less lift, improved heat transfer, and faster reaction times. With increasing M , Gr , and δ the Nusselt number increases, but it decreases with growing M and Pr . Increases in the Nusselt number indicate changes in the convective heat transfer coefficient, variations in the thickness of the thermal boundary layer, and augmentation or decrease of heat transmission. The repercussions include variations in surface temperature and an increase or reduction in the rate of heat transfer. The Sherwood number coefficient increases with growing m , Pr , Gr , and δ , but it decreases with increasing M and Ec . A greater convective mass transfer coefficient and a thinner concentration boundary layer are implied by an increase in Sherwood number. Faster response speeds and increased absorption efficiency are among the effects' after effects.

Table 1. Comparison of results of heat transfer rate

Pr	Yih [30]	Ali [31]	Reddy [32]	Present study
0.71	0.8086	0.8086	0.8086	0.8085
1	1	1	1.0001	1.0002
3	1.9237	1.9237	1.9230	1.9239

Table 2. Variations of physical parameters

m	M	Pr	Ec	δ	Gr	$f''(0)$	$g'(0)$	$-\theta'(0)$
2						0.1402	0.0215	1.3041
4	0.2	0.72	3	0.5	8	0.1504	0.0173	1.3062
6						0.1538	0.0130	1.3068
	0.1					0.1520	0.0100	1.3065
	0.2					0.1467	0.0199	1.3054
	0.3					0.1414	0.0298	1.3044
		0.5				0.1749	0.0200	1.2158
		0.72				0.1467	0.0199	1.3054
		2				0.0074	0.0192	1.7761
			0.3			0.1469	0.0199	1.3048
			3			0.1522	0.0199	1.2821
			6			0.1582	0.0199	1.2621
					5	0.1467	0.0199	1.3054
					8	0.9525	0.0223	1.3335
					10	1.4777	0.0239	1.3513
				0.1		0.1467	0.0199	1.3054
				0.5		0.2493	0.0203	1.3100
				1		0.5682	0.0216	1.3242

CONCLUSION

In this study, we explore the impact of the Hall current on the MHD boundary layer flow of a compressible viscous fluid over a stretching sheet, considering the effects of viscous dissipation.

The investigation yields the following findings:

- The temperature flow patterns, along with the primary and secondary velocity flow patterns, decreases as the Prandtl number rises.
- The temperature distribution and secondary velocity flow patterns both rise when the magnetic parameter increases, whereas the primary velocity flow patterns falls.
- Higher primary velocity flow pattern is achieved at the expense of decreased secondary velocity and temperature flow patterns when the Hall current parameter is increased.
- The primary and secondary velocity flow patterns rise with an increase in Grashof number, but the temperature gradients fall.

- As m , Ec , Gr , and δ increase, skin friction increases; as M and Pr increase, skin friction decreases.
- The Nusselt number rises as M , Gr , and δ increase but falls when m and Pr increase.
- As m , Pr , Gr , and δ increase, the Sherwood number coefficient rises; however, as M and Ec increase, it falls.

These studies have far too many potential applications. They include; examining how Hall currents affect MHD boundary layer flow of non-Newtonian fluids; analyzing how hall currents affect MHD boundary layer flow of nanofluids with viscous dissipation; examining how hall currents affect MHD boundary layer flow through porous media with a stretching sheet; examining unsteady MHD boundary layer flow with Hall currents, viscous dissipation, and a stretching sheet; and developing and comparing effective numerical methods.

AUTHORSHIP CONTRIBUTIONS

Authors equally contributed to this work.

DATA AVAILABILITY STATEMENT

The authors confirm that the data that supports the findings of this study are available within the article. Raw data that support the finding of this study are available from the corresponding author, upon reasonable request.

CONFLICT OF INTEREST

The author declared no potential conflicts of interest with respect to the research, authorship, and/or publication of this article.

ETHICS

There are no ethical issues with the publication of this manuscript.

STATEMENT ON THE USE OF ARTIFICIAL INTELLIGENCE

Artificial intelligence was not used in the preparation of the article.

NOMENCLATURE

$$Gr^* = \frac{g^* \beta^* (\bar{T}_w - \bar{T}_\infty)}{u_0^2} = \text{Grashof Number}$$

$$M = \frac{\mu_e \sigma B_0^2 x}{u_0 \rho} = \text{Magnetic parameter}$$

σ = Electrical conductivity

μ_e = Viscosity of the fluid

$m = \omega e \tau_e$ Hall parameter

$\delta = C/B$ = Velocity Parameter

$\lambda = \cos \alpha$

E = Intensity of electric field

n_e = Electron number density

E = Intensity of electric field

ν = Kinematic Viscosity

k = Thermal conductivity

u_e = External velocity

$\bar{B}_0 = \frac{B}{\sqrt{x}}$ = Magnetic field parameter

$$Ec = \frac{u_0^2}{c_p (\bar{T}_w - \bar{T}_\infty)} = \text{Eckert number}$$

Nu = Nusselt number

ρ = Density of fluid

β = Volumetric coefficient of thermal expansion

C_p = Specific heat capacity at constant pressure

A = constant

l = length

$$C_{fx} = \frac{\tau_{wx}}{\frac{1}{2} \rho u_0^2} = \text{Shear stress component due to primary velocity}$$

$$C_{fz} = \frac{\tau_{wz}}{\frac{1}{2} \rho u_0^2} = \text{Shear stress component due to secondary velocity}$$

$$\tau_{wx} = \mu \left. \frac{\partial u}{\partial y} \right|_{y=0} = \mu u_0 \left(\frac{B}{\nu} \right)^{\frac{1}{2}} f''(0) = \text{Skin friction due to primary velocity}$$

$$\tau_{wz} = \mu \left. \frac{\partial w}{\partial y} \right|_{y=0} = \mu u_0 \left(\frac{B}{\nu} \right)^{\frac{1}{2}} g'(0) = \text{Skin friction due to secondary velocity}$$

$$Nu_x = \frac{x q_w}{k (\bar{T}_w - \bar{T}_\infty)} = \text{Nusselt number}$$

REFERENCES

- [1] Yang KT, Jerger EW. First-order perturbations of laminar free-convection boundary layers on a vertical plate. *J Heat Transf* 1964;86:107–114. [\[CrossRef\]](#)
- [2] Ostrach S. An analysis of laminar free-convection flow and heat transfer about a flat plate parallel to the direction of the generating body force. In: *Radiation Heat Transfer, Augmented Edition*. London: Routledge; 2018.
- [3] Henkes RAWM, Hoogendoorn CJ. Laminar natural convection boundary-layer flow along a heated vertical plate in a stratified environment. *Int J Heat Mass Transf* 1989;32:147–155. [\[CrossRef\]](#)
- [4] Elbashbeshy EMA. Laminar boundary layer flow along a stretching cylinder embedded in a porous medium. *Int J Phys Sci* 2012;7. [\[CrossRef\]](#)
- [5] Sakiadis BC. Boundary-layer behavior on continuous solid surfaces: I. Boundary-layer equations for two-dimensional and axisymmetric flow. *AIChE J* 1961;7:26–28. [\[CrossRef\]](#)
- [6] Jha BK, Samaila G. Variable viscosity effect on boundary layer flow along continuously moving plate with the thermal boundary condition of the third kind. *Int J Appl Comput Math* 2021;7. [\[CrossRef\]](#)
- [7] Cess RD. The interaction of thermal radiation with free convection heat transfer. *Int J Heat Mass Transf* 1966;9:1269–1277. [\[CrossRef\]](#)
- [8] Soundalgekar VM, Vighnesam NV, Pop I. Combined free and forced convection flow past a vertical porous plate. *Int J Energy Res* 1981;5:215–226. [\[CrossRef\]](#)
- [9] Singh AK. MHD free-convection flow past an accelerated vertical porous plate in a rotating fluid. *Astrophys Space Sci* 1984;103:155–163. [\[CrossRef\]](#)
- [10] Kim YJ. Unsteady MHD convective heat transfer past a semi-infinite vertical porous moving plate with variable suction. *Int J Eng Sci* 2000;38:833–845. [\[CrossRef\]](#)
- [11] Bhavana M, Kesavaiah DC, Sudhakaraiyah A. The Soret effect on free convective unsteady MHD flow over a vertical plate with heatsource. *Int J Innov Res Sci Eng Technol* 2013;2:1617–1628.
- [12] Ferdows M, Ota M. Similarity solution for MHD flow through vertical porous plate with suction. *J Comput Appl Mech* 2005;6:15–25.
- [13] Crane LR. Flow past a stretching plate. *Z Angew Math Phys* 1970;21:645–647. [\[CrossRef\]](#)

- [14] Subhashini SV, Sumathi R, Pop I. Dual solutions in a thermal diffusive flow over a stretching sheet with variable thickness. *Int Commun Heat Mass Transf* 2013;48:61–66. [\[CrossRef\]](#)
- [15] Wang CY. Analysis of viscous flow due to a stretching sheet with surface slip and suction. *Nonlinear Anal Real World Appl* 2009;10:375–380. [\[CrossRef\]](#)
- [16] Wang CY. Flow due to a stretching boundary with partial slip—an exact solution of the Navier–Stokes equations. *Chem Eng Sci* 2002;57:3745–3747. [\[CrossRef\]](#)
- [17] Sparrow EM. *Radiation Heat Transfer*. Augmented Edition. Taylor & Francis; 2017.
- [18] Hady FM, Mohamed RA. Mixed convection-radiation interaction heat transfer in boundary-layer over a semi-infinite flat plate embedded in porous medium with a transfer magnetic field. *Appl Math Comput* 1994;66:103–128. [\[CrossRef\]](#)
- [19] Krishnaprakas CK. Radiation heat transfer in a participating medium bounded by specular reflectors. *Int Commun Heat Mass Transf* 1998;25:1181–1188. [\[CrossRef\]](#)
- [20] Soundalgekar VM, Patil MR, Takhar HS. MHD flow past a vertical oscillating plate. *Nucl Eng Des* 1981;64:43–48. [\[CrossRef\]](#)
- [21] Samad MA, Karim ME, Mohammad D. Free convection flow through a porous medium with thermal radiation, viscous dissipation and variable suction in presence of magnetic field. *Bangladesh J Sci Res* 2010;23.
- [22] Sattar A, Hossain M. Unsteady hydromagnetic free convection flow with Hall current and mass transfer along an accelerated porous plate with time-dependent temperature and concentration. *Can J Phys* 1992;70:369–374. [\[CrossRef\]](#)
- [23] Beg OA, Bhargava R, Rawat S, Takhar HS, Beg TA. A study of steady buoyancy driven dissipative micro polar free convection heat and mass transfer in a darcian porous regime with chemical reaction. *Nonlinear Anal Model Control* 2007;12:157–180. [\[CrossRef\]](#)
- [24] Mahatha BK, Nandkeolyar R, Mahato GK, Sibanda P. Dissipative effects in hydromagnetic boundary layer nanofluid flow past a stretching sheet with Newtonian heating. *J Appl Fluid Mech* 2016;9:1977–1989. [\[CrossRef\]](#)
- [25] Hayat T, Hendi FA. Thermal-diffusion and diffusion-thermo effects on MHD three-dimensional axisymmetric flow with Hall and ion-slip currents. *J Am Sci* 2012;8:284–294.
- [26] Marin M. On existence and uniqueness in thermoelasticity of micropolar bodies. *C R Acad Sci Paris Ser II* 1995;321:475–480.
- [27] Marin M. Some estimates on vibrations in thermoelasticity of dipolar bodies. *J Vib Control* 2010;16:33–47. [\[CrossRef\]](#)
- [28] Marin M. Lagrange identity method for microstretch thermoelastic materials. *J Math Anal Appl* 2010;363:275–286. [\[CrossRef\]](#)
- [29] Ferdows M, Ahmed AA, Tzirtzilakis E. Hall current and viscous dissipation effects on boundary layer flow of heat transfer past a stretching sheet. *Int J Appl Comput Math* 2017;3:3471–3487. [\[CrossRef\]](#)
- [30] Yih KA. Free convection effect on MHD coupled heat and mass transfer of a moving permeable vertical surface. *Int Commun Heat Mass Transf* 1999;26:95–104. [\[CrossRef\]](#)
- [31] Ali FM, Nazar R, Arifin NM, Pop I. Effect of Hall current on MHD mixed convection boundary layer flow over a stretched vertical flat plate. *Meccanica* 2011;46:1103–1112. [\[CrossRef\]](#)
- [32] Reddy MV. Influence of thermal radiation, viscous dissipation and Hall current on MHD convection flow over a stretched vertical flat plate. *Ain Shams Eng J* 2014;5:169–175. [\[CrossRef\]](#)